-RESEARCH PAPER-

International Journal of Mining and Geo-Engineering

IJMGE

IJMGE 57-1 (2023) 101-109

DOI: 10.22059/IJMGE.2022.343687.594973

A rock engineering system approach to estimate blast-induced peak particle velocity

Patrick Adeniyi Adesida [a, *]

[a] *Department of Mining Engineering, Federal University of Technology, Akure Nigeria*

Article History:
Received: 27 May 2022
Revised: 14 October 2022
Accepted: 03 November 2022

ABSTRACT

This paper presents a novel rock engineering system (RES) based method for estimating blast-induced vibration attenuation risk index and predicting peak particle velocity (PPV). The RES approach involves three key steps, which are the identification of influencing parameters, the construction of an interaction matrix, and the rating of parameters based on their influence on ground vibration. The selected parameters are the scale distance (SD), the ratio of the scale distance to stemming divided by the burden (SD/TB), the distance of the monitoring station (D), the scale distance divided by the burden (SD/B), the ratio of the scale distance to powder factor (SD/PF) and the ratio of scale distance to spacing divided by the burden (SD/SB). The results indicated that all the six parameters considered have statistically significant influences on the constructed interaction matrix system, with the SD having the highest weighty factor (21.43%) while SD/TB is the lowest (14.29%). The maximum rating of the parameters is 5, 5, 4, 5, 5, and 4 for SD, D, SD/B, SD/PF, SD/SB, and SD/TB, respectively. The attenuation risk index ranges from 14.29 to 63.43, and the slope of the actual measured PPV against the calculated attenuation risk index is negative. The developed RES-based model demonstrated better performance and a reliable method for ground vibrations prediction with a higher degree of accuracy, considering its higher determination coefficient (R2 = 0.96) and smaller error (RMSE = 1.08, MAD = 0.79, MAPE = 9.95) compared to multiple regression, Langefors & Kihlstrom and Hudaverdi models.

Keywords: *Attenuation risk index, Blasting, Ground vibration, Peak particle velocity, Rock engineering system, Scale distance*

1. Introduction

Fragmentation of rocks for aggregate production, loosening of minerals from parent rocks, extraction of ore, and other civil works without impairing the immediate environment have been the concern of blast engineers for a long time. Blasting is the primary method of rock fragmentation, and it causes ground vibration, fly rocks, air-blast and back-break, which are unwanted phenomena that cause damage to the environment. Despite these unwanted occurrences from blasting, it is still the most used method of rock fragmentation because it is cost-effective and highly efficient [1], depending on the technical know-how of blasters and the understanding of the geological properties of rocks. There seems to be no acceptable and environmentally friendly method of rock fragmentation than blasting. Hence, the need to manage and control the unwanted situations resulting from it in mines and quarries. Some blasters had used their experience and the trial-by-error method to mitigate the side effects of blasting and had succeeded over time [2]. The increase in the population of most cities and subsequent expansion has reduced the proximity of mines and quarries to those cities. Therefore, it is necessary to redesign blasting to reduce its environmental impact.

Researchers regard blast-induced ground vibration as one of the most devastating side effects of blasting that must be controlled and managed [3]. The reason is that vibration is the most felt impact, and researchers and explosive engineers are yet to provide a solution. Studies have proved that when an explosive detonates, it is done violently and generates seismic waves like earthquakes [4-5]. The seismic waves move through the cracks created in rocks and ground to cause movement of the ground particles [4]. Ground vibration is a product of dissipating energy generated by explosives for fragmentation in blasting operations [4, 6]. Evidence suggests that it does not depend only on charge quantity but also on blast design [7]. There had been a correlation between the mass of explosives for blasting, the ground vibration produced, and the monitoring distances [8, 9]. The cycle of blast-induced ground vibration waves decreases with increasing distance and increases with a higher quantity of explosives [9-13]. The effects of ground vibration include disturbance of the natural habitats of plants and animals [14], the distorted composition of groundwater [15], and the creation of crakes on the wall of buildings, among others [16].

Researchers often use frequency and the peak particle velocity of the seismic waves generated by blasting to measure blast-induced ground vibration [17]. However, the peak particle velocity (PPV), measured in millimeters per second (mm/sec) with the aid of seismographs that present the results in three dimensions, longitudinal, transverse, and vertical, are often used [18]. The United States Bureau of Mines (USBM) proposed that the maximum allowable PPV that structures on soil near mine areas can withstand is 60 mm/second. Those on the weak rock are 110 mm/second and 230 mm/second PPV for those on the hard rock [19-21]. The improvement of blast design for effective blast-induced ground vibration management needs an accurate prediction of PPV and an understanding of how blast-design parameters such as spacing and burden interact to influence the degree of blast-induced ground vibration. However, the most acceptable blast-induced ground vibration predictive model is the USBM model developed by Duvall and Fogleson [22]. Other early predictors of blast-induced ground vibrations are Langefors and Kihlstrom [23], Ambraseys and Hendron [24], and the

* Corresponding author. *E-mail address:* paadesida@futa.edu.ng (P. A. Adesida).

Indian Standards Institute [25]. Recently, several researchers have worked on developing models for predicting blast-induced ground vibrations using various methods such as multivariate analysis [8] and artificial neural networks [8, 20-21, 26-28]. Ajaka and Adesida [29] attempted to evaluate the influence of rock properties on blast-induced ground vibrations by comparing blast-induced PPV values in a limestone quarry to that of a dolomite quarry. Hacefendioglu [13] analyzed the spatial variation of blast ground motion to examine its effects on stochastic responses of short-span highway bridges. However, some other researchers proved that these models could not predict accurately at all times and everywhere [20, 30]. Hence, the need for improvement of the models and development of other models for better prediction of PPV or frequency of ground vibration.

This study aimed to estimate blast-induced ground vibration's attenuation risk index and predict PPV using the rock engineering system (RES) approach. The RES method has been applied to solve varieties of engineering problems, for instance, the investigation of the effects of spent fuel disposal on the environment [31], the studying of ecosystems [32-33], the assessment of radioactive waste control [34-35], traffic-induced air pollution [35] and environmental risk associated with reservoir pollution [36]. Recently, the RES approach was applied to research multiple rock engineering problems, such as the calculation of the rate of penetration for tunnel boring machines [37], estimation of safety factors for circular failure [38], evaluation of shaft resistance of a pile entrenched in rock [39] and the prediction of rock mass deformation modulus [40]. Also, Adesida [2] used the RES approach to predict powder factors using rock mass and geometric parameters, while Huang et al. [41] used it to classify rock mass. Fattahi [42] used the RES to assess the rotational torque needed for horizontal directional drilling. Also, Faramarzi et al. [43] used RES to predict the distance of flyrock in surface blasting, while Saffari et al. [44] used it to investigate the potential of spontaneous combustion of coal. However, no researcher has explored the use of the Rock Engineering System (RES) method to predict PPV and explore how the parameters that influence blast-induced ground vibration interact.

This study focussed on blast-induced vibration attenuation risk index (*Ari*) estimation and a new PPV predictive model development using the RES approach. The RES model is structured to accommodate as many influencing parameters as possible. The RES approach also has the advantage of analyzing descriptive parameters over the ANN and other methods. The model was developed based on data in open-source literature from the study of Hudaverdi [8]. Performance comparative analysis was done for the RES, multiple regression, Langefors & Kihlstrom, and Hudaverdi models using the coefficient of determination values (R^2) and error analysis (RMSE, MAD, and MAPE).

2. The Rock engineering system (RES)

The RES is an essential tool for illustrating those parameters with a high degree of influence in problems associated with rock engineering [45-46]. The RES approach involves three key steps, which are the identification of influencing parameters, the construction of an interaction matrix, and the rating of parameters based on their influence. The interaction matrix utilized for describing the key parameters and their interaction in the RES structure is the major component of the RES approach. The interaction matrix is structured such that the primary parameters influencing the system are along the central diagonal of the matrix structure. The coded values recording their degree of interaction are in the perpendicular cells in the matrix. The description of a two-parameter matrix structure and the broad idea of coding the interaction matrix structures are shown in Figures 1 and 2, respectively.

There are five methods of coding in the interaction matrix structure. These methods are expert semi-quantitative (ESQ), binary, continuous quantitative coding (CQC) [45, 47-50], probabilistic expert semi-quantitative (PESQ), and expert method [44]. However, the ESQ method is more used than others because it is easy to understand. Likewise, in this paper, the ESQ method for assigning code to the relationship between parameters in the interaction matrix, as described by Hudson [45], was used. The interaction intensity's description is by number representation, where 0 means no interaction, 1 is weak interaction, 2 is medium interaction, 3 represents strong, and 4 to critical interaction [43, 45]. Moreso, the advantage of this method is that the number of parameters in the interaction matrix has no limitations [52].

Coding the interaction of parameters in the matrix structure is done by inserting the number of the weight of the interaction of two parameters in their perpendicular cell. The sum of the horizontal values of each parameter in the structure is the measure of the influence of the individual parameter on the matrix structure, called the Cause (C_i) of the parameter (Equation 1). The sum of the vertical values measures the influence of the matrix structure on the parameter, and it is known as the Effect (E_i) of the parameter (Equation 2) [53]. The addition and subtraction of the Cause and Effect of each parameter is the measure of their significance in the interaction matrix, known as the interactive intensity and dominance, respectively. Parameters significance analysis for the interaction matrix structure is by plotting the coordinate values of Effect against Cause. A diagonal line on the cause-effect plot denotes points of equal value of Causes and Effects, which signifies the locus point where their dominance and subordination for all parameters are at equilibrium. Parameters on the right side of the diagonal line are those with more value of Causes than Effects, known as the dominant parameters. While those with lesser Causes than their Effects are on the left-hand side and are subordinate parameters. The weight factor (α_i) of each parameter in the system, which is the percentage sum of Cause and Effect, is calculated using Equation 3 [45-46, 53-54].

$$C_{pi} = \sum_{j=1}^{n} I_{ij} \quad (1)$$

$$E_{pj} = \sum_{i=1}^{n} I_{ij} \quad (2)$$

$$\alpha_i = \frac{(C_i + E_i)}{(\sum_i C_i + \sum_i E_i)} \times 100 \quad (3)$$

where C_i is the cause of the ith parameter, and E_i is the effect of the ith parameter.

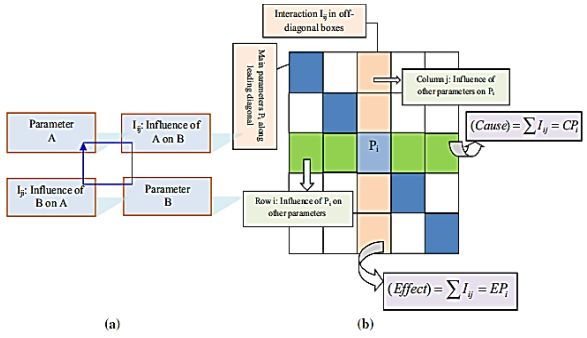

Figure 1. The principle of the interaction matrix in RES, (athe) two parameters (b) unlimited parameters [45, 55].

3. Methodology

3.1. Narrative of the adopted group of datasets

The specific objective of this paper is to develop a RES-based predictive model for the estimation of PPV using the knowledge of interaction among parameters that influence ground vibration. The interaction matrix development involves the blast geometry, the distance between the monitoring stations and the blast centers, data obtained from seismographs, and the rating of the influence of each parameter on PPV to develop the RES model. Data for this study were from the field investigations conducted by Hudaverdi [8] in Akdaglar Quarry, Istanbul, Turkey. Aggregate production for asphalt and concrete works is the operation of the quarry. The measurement of PPV in the quarry in the study is by Instantel tri-axial seismographs. The specification of the seismograph is 0.127–0.0159 mm/s resolution, a sampling rate of 1024 samples/s, and an accuracy of 3% at 15 Hz. The

PPV values measured by the seismograph vary from 0.127 mm/s to 254 mm/s at a frequency of 2 to 300 Hz. The geometric parameters of the blast design, such as the drilled-hole diameter, burden, spacing, sub-drill, hole depth, stemming, and specific charge, were measured. In the study, Hudaverdi [8] modified the USBM PPV prediction model by using multivariate analysis to predict PPV, using a total of eighty-eight (88) datasets generated. The datasets were classified into two homogeneous groups according to similarity using cluster analysis, and the evaluation and confirmation of the group members were by using discriminant analysis. The development and validation of the RES-based model for predicting PPV in this paper were through datasets from one of the clustered groups.

3.2. The RES application to PPV prediction

Ratios of the blast design parameters and the monitoring distance of the PPV measured in thirty blasts by Hudaverdi [8] were used to develop scale distances and other factors identified to influence PPV. Blast design parameters are often considered in ratios because they are interrelated and depend on hole diameter [56]. In this study, the burden (B), powder factor (PF), the ratio of spacing to that of burden (SB), that of stemming to the burden (TB), and quantity of charge (Q) were the blast design parameters considered. The parameters also include measured distances between the monitoring stations and the center of blasts (D). The scale distance (SD) was estimated using the ratio of D to the square root of Q. Powder factor (PF) is adjudged an important blast design parameter by blast engineers and was considered for this study because of its influence on ground vibration [57]. Inadequate PF will cause the overloading of explosives and excessive ground vibration [58]. SB ranges from 1 to 2 depending on the energy coverage of a bench [8]. Detonation of explosives when S is less or too high than B may cause early splitting between blast holes and subsequent premature fragmentation of the stemming. These scenarios lead to a quick release of gases, causing excessive ground vibration and back-break, which result in poor fragmentation [59-60]. Generally, the value of TB is around 1. When TB is low, or the stemming length is too high, it may cause premature release of explosive gases, which results in poor rock fragmentation, and flyrock and increase the propagation of the seismic wave [60]. The burden is an essential individual parameter in blast design considered in this study because of its importance to the propagation of blast-induced ground vibration. A small B allows gas from detonated explosives to escape quickly to the atmosphere, causing air blasts and noise pollution [57-58]. However, a large B confines gases and may result in ground vibrations and back-break. In this study, the RES model was optimized, using the ratios of SD to PF, B, SB, and TB together with D and SD to develop a PPV predictive model. The rationale for selecting these parameters is their strong relationship with measured PPV.

The attenuation risk index (*Ari*) estimation and PPV prediction were by modeling the interaction of the parameters with the RES approach. The influence of these parameters on PPV was studied meticulously and used to create an interaction matrix for the weighty factor (α) development for each parameter used for the RES prediction model for PPV. The fundamental parameters are the measured PPV, distances between the monitoring station and the center of the blast (D), the charge per delay (Q), and the burden (B). Derived parameters were the scale distances (SD) and the ratio of scale distance to stemming divided by the burden (SD/TB). The scale distance is the ratio of the D to the square root of Q. Other parameters derived are the scale distance divided by the burden (SD/B), the scale distance divided by the powder factor (SD/PF), and the ratio of scale distance to spacing divided by the burden (SD/SB). The six final parameters for the RES-based PPV prediction model development are D, SD, SD/TB, SD/PF, SD/B, and SD/SB (Table 1)..

3.3. Rating of parameters

Parameters were rated using their classes and how they influence blast-induced ground vibration. The rating of parameters starts from zero (0) to ends at a specific positive figure depending on the number of classes. The rating is such that if a parameter has four groupings, the rating will start from 0 to 3. Zero indicates the worst condition of influence of the parameter on PPV, while 3 signifies the best conditions. In other words, it is an unfavorable or poor effect on the propagation of PPV, and 3 indicates the most favorable conditions. The rating proposed in this study was by experience in rock blasting and excavation, outputs of other work, and estimation of existing ratings to find the proposed ratings for various ratios used in the study.

3.4. Estimating PPV attenuation risk index

Adesida [2] adopted the method used by Bernados and Kaliampakos [54], Faramarzi et al. [51], and Hasanipanah et al. [61] for the estimation of the vulnerability index (VI) of rock fragmentation, which is the risk in fragmentation (poor fragmentation), to develop the powder factor risk index in his study, as shown in Equation 4. The Pfi is the risk associated with the powder factor (poor blast design), correlated with the measured powder factor to develop the RES-based predictive model.

$$Pfi = 100 - \sum_{i=1} \alpha_i \frac{Q_i}{Q_{max}} \quad (4)$$

Where α_i, Q_i, and Q_{max} are the weighty factor, the value (rating), and the max value assigned for the i^{th} parameter, respectively. 100 is the highest value allocated to Pfi, which is the powder factor's worst-case scenario. In contrast, zero, the lowest value, indicates the most favorable condition for the powder factor. This study implemented the same approach for estimating PPV's attenuation risk index (*Ari*). A_{ri} is the measure of the combined risk associated with blast-induced ground vibration. The peak particle velocity's attenuation index is estimated using Equation 5.

$$A_{ri} = 100 - \sum_{i=1} \alpha_i \frac{Q_i}{Q_{max}} \quad (5)$$

The attenuation risk index is from 0 to 100, indicating various levels of severity of the controlled scale and grouped into three categories [54], shown in Table 2.

Table 1. Description of the parameters.

Parameter	Symbol	Min	Max	Mean	SD
Distance	D	70.0	245.0	170.5	48.09
Scale distance	SD	7.74	23.34	15.44	3.66
Scale distance to burden	SD/B	3.1	9.95	6.34	1.66
Scale Distance to powder factor	SD/PF	14.34	46.69	28.90	7.45
Scale distance to spacing to burden	SD/SB	6.45	20.84	13.35	3.29
Scale distance to stemming to burden	SD/TB	6.45	20.24	14.12	3.36

Table 2. Classification of *Ari* [54]

Description	Low – Medium	Medium-High	High – Very High
Category	I	II	III
Ari	0 – 33	33 – 66	66 – 100

3.5. Error Analysis

Thirteen datasets in cluster 1 of the Hudaverdi [8] study, but not part of those used for the development of the models, were used to test the models by predicting RES, regression, Hudaverdi and Langefors and Kihlstrom. Error analysis of the estimated PPV using the RES, regression, Hudaverdi, and Langefors & Kihlstrom models was by using the training and testing datasets. The estimation of the goodness of fit of the predicted PPV was by the root mean square error (RMSE), the mean absolute deviation (MAD), and the mean absolute percentage error (MAPE) methods. Although, the RMSE provides the average error bias using the square of the error. However, RMSE cannot specify the data deviation trend but typically assign more weight to higher errors than smaller ones. Thus, RMSE is inefficient for error analysis for large

sample sizes but suitable for errors in small samples. Defiantly, the accuracy factor indicates the deviation between predictions by models and measured datasets. Theoretically, a predictive model is exceptionally accurate when RMSE is 0, R2 is 1, MAD is 0, and MAPE is 0%. The formulas for calculating RMSE, MAD, and MAPE are presented in Equations 6 - 8.

$$RMSE = \sqrt{\frac{1}{n}\sum_{i=1}^{n}\left(X_{i\,(meas)} - X_{i\,(pred)}\right)^2} \quad (7)$$

$$MAD = \frac{1}{n}\sum_{i=1}^{n}\left|X_{i\,(meas)} - X_{i\,(pred)}\right| \quad (8)$$

where Xi (meas) and Xi (predi) are measured and predicted variables, respectively, while n is the number of observations.

4. Results and discussion

4.1. Development of interaction matrix

The influence of one parameter on another was investigated and coded using the expert semi-quantitative method and presented in Table 3. The six parameters used for the peak particle velocity prediction were in the cells along the central diagonal of the developed matrix table. The interaction intensity (C+E), degree of dominance (C-E), and the weighty factor (Equation 3) of each of the parameters were estimated from the interaction matrix, as shown in Table 4. The result indicated that the scale distance has the highest interaction significance in the interaction matrix system. The ratio of scale distance to that of the stemming to the burden has the lowest significant level. More so, the range of values (20-30) for the interaction intensity in the matrix shows that all the parameters have a statistically significant influence on the system. The results of the interaction intensity of the individual parameter are in Figure 2.

Table 3. Interaction Matrix.

SD	2	4	2	1	2
3	**D**	1	1	2	0
4	3	**SD/B**	3	4	3
4	3	1	**SD/PF**	1	0
4	3	0	4	**SD/SB**	1
4	3	1	2	4	**SD/TB**

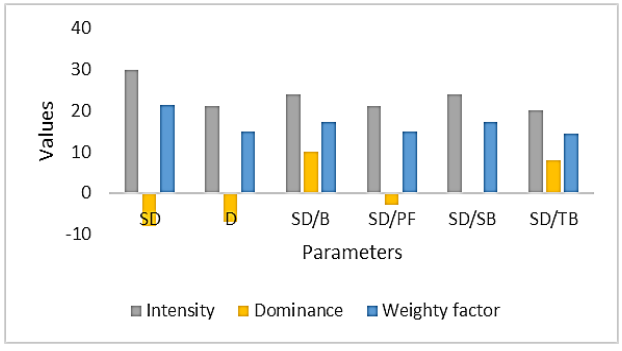

Figure 2. Interaction Intensity of the parameters.

According to Hudson [45], the line C=E on the C-E plot, shown in Figure 3, are points where the cause is equivalent to the effect. The points over the C=E line are known as the dominants, while those under it are called the subordinates. That is, parameters above the C=E plots are dominant, while those under them are subordinate in the system. The dominant parameters in the system are D, SD, and SD/PF. The SD/B and SD/TB are subordinate in the system. The SD/SB is at equilibrium in the system.

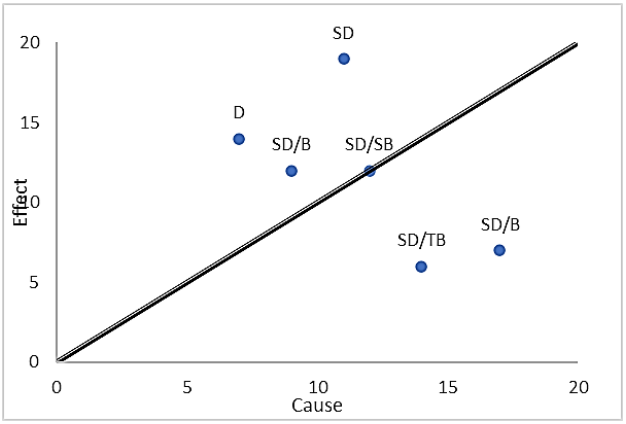

Figure 3. Cause and Effect plot.

Table 4. The weighting factor of the parameters.

Parameter	C	E	C+E	C-E	α_i (%)
SD	11	19	30	-8	21.43
D	7	14	21	-7	15.00
SD/B	17	7	24	10	17.14
SD/PF	9	12	21	-3	15.00
SD/SB	12	12	24	0	17.14
SD/TB	14	6	20	8	14.29
Sum	**70**	**70**	**140**	**0**	**100**

4.2. Rating of parameter

Table 5 presents the rating of individual parameters based on how they influence ground vibration. The range of values indicates the influence of each value on blast-induced ground vibrations. The result shows that the SD, D, SD/PF, and SD/SB have a maximum rating of 5. The SD/TB and SD/B have 4. The belief is that parameters with the highest rating will have an increased influence on blast-induced ground vibration propagation.

Table 5. Ratings for parameters influencing PPV.

Parameter	Values and Ratings					
SD	<5	5-10	10-15	15-20	20-25	>25
Rating	5	4	3	2	1	0
D	<100	100-200	200-400	400-600	600-800	>800
Rating	5	4	3	2	1	0
SD/B	<5	5-10	10-15	15-20	>20	
Rating	4	3	2	1	0	
SD/PF	<10	10-15	15-20	20-25	25-30	>30
Rating	5	4	3	2	1	0
SD/SB	<5	5-10	10-15	15-20	20-25	>25
Rating	5	4	3	2	1	0
SD/TB	<5	5-10	10-15	15-20	>20	
Rating	4	3	2	1	0	

4.3. 3 Ground vibrations' attenuation risk index

The estimated attenuation risk index for each parameter was by their calculated weighty factor, the assigned maximum rating, and the exact rating based on their measured values. The estimated *Ari* for each recorded blast ranges from 14.29 to 63.43 (Table 6). It indicates that the attenuation risk index for the observed datasets ranges from low-medium to medium-high. The slope of the peak particle velocity against the calculated attenuation risk index shows that the index reduces with the PPV. It means that the blast-induced ground vibrations from excess explosive usage during blasting operations reduce with increased damping or attenuation factor. Therefore, the first category of the attenuation risk index, which ranges from 0 to 33,

indicates a low damping factor, which will result in a high degree of damage to structures and the environment within the radius of the measured distance. The second category ranges from 33 to 66, which indicates moderate problems associated with ground vibration, that may impact the environment. The third category ranges from 66 to 100. It is a high attenuation damping factor that may not affect structures within the radius of the measured distance and the environment at large. The findings agree with previous studies that ground vibration reduces with distance [10, 33].

Table 6. Estimated attenuation risk index (*Ari*) for the monitored blasts.

Blast No	SD	D	SD/B	SD/PF	SD/SB	SD/TB	A_{ri}
3	4	5	4	4	4	3	14.29
9	3	4	3	1	3	2	41.86
10	2	4	3	0	3	1	52.72
12	2	4	3	0	2	0	59.72
16	2	3	3	1	3	0	56.29
18	2	4	3	1	3	1	49.72
21	2	3	3	0	2	0	62.72
33	3	4	3	2	3	2	38.86
35	1	3	3	0	2	1	63.43
36	3	4	3	1	3	3	38.29
39	3	4	3	2	3	2	38.86
41	2	3	3	0	2	1	59.14
44	4	5	4	3	4	3	17.29
47	2	3	3	0	3	2	52.14
48	3	4	4	3	4	3	24.57
52	2	3	3	0	2	1	59.14
55	3	4	3	1	3	2	41.86
63	3	4	4	2	2	3	34.43
66	3	4	4	3	4	3	24.57
69	3	4	3	2	3	2	38.86
70	1	3	3	0	2	1	63.43
71	2	3	3	1	3	1	52.72
73	2	3	3	0	3	2	52.14
74	3	4	3	2	3	2	38.86
77	3	4	3	1	3	2	41.86
78	1	4	3	0	2	1	60.43
79	2	4	3	1	3	1	49.72
84	3	4	3	1	3	2	41.86
85	3	4	3	1	3	2	41.86
87	3	4	4	2	3	2	34.57
Q_{max}	5	5	4	5	5	4	
α_i	21.43	15	17.14	15	17.14	14.29	100

4.4. The RES-based PPV prediction model

The RES model for PPV prediction development is a linear regression statistic model between the measured PPV and the estimated attenuation risk index (*Ari*). The model is represented mathematically in Equation 9. The coefficient of correlation (R^2) for this model is 0.96 (Figure 4), which is a good relationship, while the correlation between the measured and predicted PPV is in Figure 5.

$$PPV = 28.311 - 0.4026A_{ri} \quad (9)$$

where *Ari* is the attenuation risk index, and PPV is the peak particle velocity in mm/s.

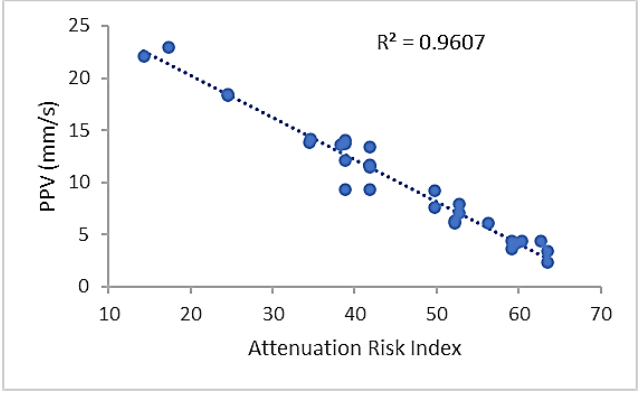

Figure 4. PPV predictive model using Ari.

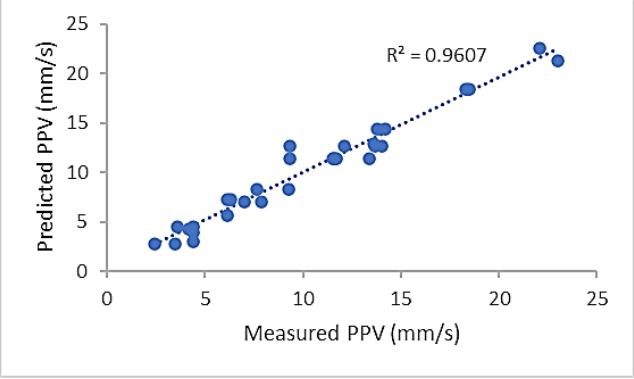

Figure 5. The predicted PPV against the Measured PPV.

4.5. Validation of the Proposed RES model

The validation of the RES-based model for the prediction of PPV developed in this study was by comparing it with the multivariable linear regression, Hudaverdi, Langefors, and Kihlstrom models. And by evaluating the error analysis of the models using testing datasets. The training datasets used in this study were analyzed using multivariable regression statistics to formulate a mathematical predictive model for PPV with the aid of SPSS software and the model shown in Equation 10. The coefficient of determination of the regression statistic is 0.88, while the analysis of variance shows that the regression is statistically significant at 1.32E-09. The predicted PPV using the testing datasets for the RES, regression, Hudaverdi, Langefors, and Kihlstrom models are shown in Table 7, while the comparison of the error analysis for the models is in Table 8. For the training datasets, the RES-predicted PPV has the least values for RMSE, MAD, and MAPE, while for the testing datasets, the Hudaverdi model has the least error values for the error analysis. The results of the comparison between the actual measured and predicted PPV using various models is in Figure 7. The figure shows that the RES-predicted PPV is more adaptable to the measured PPV than other predictive models.

$$PPV = 33.01 - 3.174SD - 0.017D + 2.18\frac{SD}{B} + 0.247\frac{SD}{PF} + 0.979\frac{SD}{SB} - 0.344\frac{SD}{TB} \quad (10)$$

where D is the distance of the monitoring station to the center of the blast (m), SD is the scale distance ($m/kg^{\frac{1}{2}}$), B is the burden (m), PF is the powder factor (Kg/m^3), SB is the spacing-burden ratio, and TB is the ratio of stemming to burden.

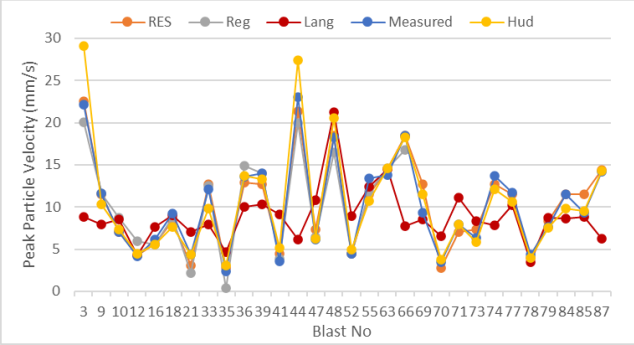

Figure 7. Comparison of measured PF with RES and regression predicted PF.

5. Conclusion

Rock blasting activities in the proximity of urban areas require special monitoring to reduce complaints and litigations, thus, improving the protection of natural resources and infrastructures. Hence, the RES model presented in this study improved the estimation of ground vibration that may arise from blasting. The RES is an expert-based approach that can accommodate many input parameters. The model can also deal with the complex characteristics of geological systems often associated with inherent uncertainties. Moreover, it has an advantage over statistical modeling and ANN methods in considering descriptive input parameters. The study shows that scale distance has the highest interaction (30) in the RES matrix system, thus, the most sensitive parameter in the system. While the scale distance has the highest weighty factor in the matrix system (21.43 %), and it is highly controlling other parameters. The study has shown that the blast design parameters influence the magnitude of ground vibrations propagated during explosive detonation in blasting operations and not only the scale distance as postulated by the USBM. The slope of the peak particle velocity against the calculated attenuation risk index indicates that the index reduces with the PPV. It means that the blast-induced ground vibrations from excess explosive usage during blasting operations reduce with increased damping or attenuation factor. The attenuation risk index can be a tool for estimating the safe distance for blasting as it indicates that where the *Ari* is low, the risk of damage due to ground vibration is high.

Conclusively, the RES-based model developed for PPV prediction performs better than the multiple regression, Langefors & Kihlstrom, and Hudaverdi models with $R^2 = 0.96$, RMSE = 1.08, MAD = 0.79, MAPE = 9.95, which indicates a high performance with limited error. Therefore, RES modeling is a reliable tool for predicting ground vibrations. The developed RES model can be used to design blasts based on the maximum permissible peak particle velocity limits for infrastructures close to quarries. However, the RES-based PPV predictive model (Equation 10) developed in this paper is open for more development because it did not consider rock and soil properties. Also, the model cannot be generalized because it is site specific. Therefore, results may vary from one location to another due to uncertainties in the geological system. Future work should include rock and soil properties as input parameters in the RES model. Also, data should be from different locations in consideration of the heterogeneous nature of the geological system.

Table 7. Predicted PPV by different models for the testing datasets.

A_{ri}	Measured PPV (mm/s)	Predicted PPV (mm/s)			
		RES ($R^2 = 0.82$)	Regression ($R^2 = 0.79$)	Hudaverdi ($R^2 = 0.76$)	Langerfors ($R^2 = 0.48$)
14.29	32.10	22.56	21.35	43.71	17.26
41.86	8.20	11.46	12.54	9.31	6.97
49.14	13.20	8.53	11.78	8.36	6.49
41.86	9.13	11.46	11.71	9.78	7.98
38.86	10.50	12.67	13.04	10.42	6.94
27.57	28.00	17.21	15.13	17.67	22.70
20.29	28.30	20.14	18.55	26.94	20.64
28.15	22.40	16.98	14.60	20.35	16.79
31.15	21.00	15.77	16.11	18.12	9.34
38.86	8.41	12.67	11.82	9.40	9.27
20.29	25.10	20.14	19.75	25.98	12.26
38.86	12.20	12.67	12.64	12.55	19.34
31.00	20.4	15.83	16.68	16.26	9.73

Table 8. Error analysis of different models.

Models	Training			Testing		
	RMSE	MAD	MAPE	RMSE	MAD	MAPE
RES	1.08	0.79	9.95	5.8	5.06	28
Regression	1.47	1.16	15.26	6.5	5.37	29
Hudaverdi	1.89	1.19	11.43	4.8	3.17	10
Langefors & Kihlstrom	5.37	3.77	40.00	8.16	6.68	35

REFERENCES

[1] Zhang, Z., Hou, D., Guo, Z., He, Z., & Zhang, Q. (2020). Experimental study of surface constraint effect on rock fragmentation by blasting. *International Journal of Rock Mechanics and Mining Sciences,* 128, 104278. doi: https://doi.org/10.1016/j.ijrmms.2020.104278

[2] Adesida, P. A. (2022). Powder factor prediction in blasting operation using rock geo-mechanical properties and geometric parameters. *International Journal of Mining and Geo-engineering;* 56(1), 25-32. doi: https://doi.org/10.22059/IJMGE.2021.310930.594870

[3] Rodríguez, R., García de Marina, L., Bascompta, M., & Lombardía, C. (2021). Detsermination of the ground vibration attenuation law from a single blast: A particular case of trench blasting. *Journal of Rock Mechanics and Geotechnical Engineering,* 13(5), 1182–1192. doi: https://doi.org/10.1016/j.jrmge.2021.03.016

[4] Lopez-Jimeno, C. L., Jimeno, E., & Carcedo, F. J. A. (1995). Drilling and Blasting of Rocks Rotterdam: A. A. Balkema Publishers.

[5] Hammed, O. S., Popoola, O. I., Adetoyinbo, A. A., Awoyemi, M. O., Adagunodo, T. A., Olubosede, O., & Bello, A. K. (2018). Peak particle velocity data acquisition for monitoring blast induced earthquakes in quarry sites. *Data in Brief,* 19, 398-408. doi: https://doi.org/10.1016/j.dib.2018.04.103

[6] Dumakor-Dupey, N. K., Arya, S., & Jha, A. (2021). Advances in Blast-Induced Impact Prediction—A Review of Machine Learning Applications. *Minerals,* 11(6), 601-630. doi: https://doi.org/10.3390/min11060601

[7] Zhen-xiong, W., Wen-bin, G., Ting, L., Jian-qing, L., Jing-lin, X., & Xin, L. (2016). Blasting Vibration Generated by Breaking-Blasting Large Barriers with EBBLB. *Shock and Vibration,* 1–13. doi: https://doi.org/10.1155/2016/7503872

[8] Hudaverdi, T. (2012). Application of multivariate analysis for prediction of blast-induced ground vibrations. *Soil Dynamics and Earthquake Engineering*; 43, 300-308. doi: http://dx.doi.org/10.1016/j.soildyn.2012.08.002

[9] Hacefendioglu, K., & Alpaslan, E. (2015). Stochastically simulated blast-induced ground motion effects on non-linear response of an industrial masonry chimney. *Stochastic Environmental Research and Risk Assessment,* 28 (2) 415–427. https://doi.org/10.1007/s00477-013-0761-7

[10] Yin, Z., Hu, Z., Wei, Z., Zhao, G., Hai-feng, M., Zhang, Z., & Feng, R. (2018). Assessment of Blasting-Induced Ground Vibration in an Open-Pit Mine under Different Rock Properties. *Advances in Civil Engineering,* 1–10. doi: https://doi.org/10.1155/2018/4603687

[11] Jayasinghe, B., Zhao, Z., Teck Chee, A. G., Zhou, H., & Gui, Y. (2019). Attenuation of rock blasting induced ground vibration in rock-soil interface. *Journal of Rock Mechanics and Geotechnical Engineering,* 11(4), 770-778. doi: https://doi.org/10.1016/j.jrmge.2018.12.009

[12] Hacefendioglu, K., & Soyluk, K. (2012). Effects of blast-induced random ground motions on the stochastic behaviour of industrial masonry chimneys. *Structural Engineering and Mechanics,* 43(6),835–845. doi: https://doi.org/10.12989/sem.2012.43.6.835

[13] Hacıefendioglu, K. (2017). Stochastic dynamic response of short-span highway bridges to spatial variation of blasting ground vibration. Applied Mathematics and Computation, 292, 194–209. https://doi.org/10.1016/j.amc.2016.07.039

[14] Rehmana, G., khattakb, I., Hamayunc, M., Rahmana, A., Haseeba, M., Umara, M., Alia, S. Iftikhard, W., Shamsa, A., & Pervaiz, R. (2021). Impacts of mining on local fauna of wildlife in District Mardan & District Mohmand Khyber Pakhtunkhwa Pakistan. *Brazilian. Journal of Biology*, 84(e251733), 1-11. doi: https://doi.org/10.1590/1519-6984.251733

[15] Gascoyne, M., & Thomas, D. A. (1997). Impact of blasting on groundwater composition in a fracture in Canada's Underground Research Laboratory. *Journal of Geophysical Research;* 102(B1), 573-584.

[16] Adepitan, R. A., Owolabi, A. O., & Komolafe, K. (2018). Prediction of structural response to blast-induced vibration in Kopek Construction Quarry, Ikere-Ekiti, Ekiti State, Nigeria. *International Journal of Environmental Studies,* 75(6), 990–999. doi: https://doi.org/10.1080/00207233.2018.1473207

[17] Saadat, M., Khandelwal, M., & Monjezi, M. (2014). An ANN-based approach to predict blast-induced ground vibration of Gol-E-Gohar iron ore mine, Iran. *Journal of Rock Mechanics and Geotechnical Engineering,* 6(1), 67–74. doi: https://doi.org/10.1016/j.jrmge.2013.11.001

[18] Lawal, A. I., & Idris, M. A. (2019): An artificial neural network-based mathematical model for the prediction of blast-induced ground vibrations. *International Journal of Environmental Studies,* 1-17. doi: https://doi.org/10.1080/00207233.2019.1662186

[19] Nicholls, H.R., Johnson, C. F., & Duvall, W. I. (1971*). Blasting Vibrations and Their Effects on Structures,* Bureau of Mines, Washington DC, 1971. Bulletin 656.

[20] Dowding, C. H. (1985). Blast Vibration Monitoring and Control, Prentice–Hall, Englewood Cliffs, NJ.

[21] Odello, R. J. (1980). Origins and Implications of Underground Explosives Storage Regulations Technical Memorandum, No. 51-80-14, Naval facilities engineering command, USA

[22] Duvall, W. I., & Fogleson, D. E. (1962). Review of criteria for estimating damage to residences from blasting vibration. Report no. 5968 (Washington, DC: United States Bureau of Mines).

[23] Langefors, U. & Kihlström, B. (1978). *The Modern Technique of Rock Blasting*. John Wiley & Sons.

[24] Ambraseys, N. R., & Hendron, A. J. (1968). Dynamic behaviour of rock masses. In: K. G. Stagg and O.C. Zeinkiewicz (Eds) Proceedings of the Rock Mechanics in Engineering Practice (London: Wiley), 203–227.

[25] Indian Standards Institute, (1973) Criteria for safety and design of structures subjected to underground blast. *ISI Bulletin* IS-6922 (New Delhi: Indian Standards Institute).

[26] Ragam, P., & Nimaje, D. S. (2018). Evaluation and prediction of blast-induced peak particle velocity using artificial neural network: A case study. *Noise & Vibration Worldwide,* 49(3), 111–119. doi: https://doi.org/10.1177/0957456518763161

[27] Dehghani, H., & Ataee-pour, M. (2011). Development of a model to predict peak particle velocity in a blasting operation. *International Journal of Rock Mechanics and Mining Sciences,* 48(1), 51–58. doi: https://doi.org/10.1016/j.ijrmms.2010.08.005

[28] Nguyen, H., Bui, X., Tran, Q., Le, T., Do, N., & Hoa, L. T.

(2019). Evaluating and predicting blast-induced ground vibration in open-cast mine using ANN: a case study in Vietnam. *SN Applied Sciences,* 1(1), 125–135. doi: https://doi.org/10.1007/s42452-018-0136-2

[29] Ajaka, E. O., & Adesida, P. A. (2014). Importance of Blast-Design in Reduction of Blast-Induced Vibrations. *International Journal of Science, Technology and Society*, 2(3), 53-58. doi: https://doi.org/10.11648/j.ijsts.20140203.14

[30] Jahed, A. D., Hajihassani, M., Mohamad, E. T., Marto, A., & Noorani, S. A. (2014). Blasting induced flyrock and ground vibration prediction through an expert artificial neural network based on particle swarm optimization. *Arabian Journal of Geosciences,* 7(12), 5383–5396. doi: https://doi.org/10.1007/s12517-013-1174-0

[31] Skagius, K., Wiborgh M., Ström A., & Morén L. (1997). Performance Assessment of the Geosphere Barrier of a Deep Geological Repository for Spent Fuel: The Use of Interaction Matrices for Identification, Structuring and Ranking of Features, Events and Processes. *Nuclear Engineering and Design,* 176(1), 155-162.

[32] Avila, R., & Moberg, L. (1999). A Systematic Approach to the Migration of< Sup> 137</Sup> Cs in Forest Ecosystems Using Interaction Matrices. *Journal of Environmental Radioactivity,* 45(3), 271-282.

[33] Velasco, H., Ayub, J., Belli, M., & Sansone, U. (2006). Interaction Matrices as a First Step Toward a General Model of Radionuclide Cycling: Application to the 137 Cs Behavior in a Grassland Ecosystem. *Journal of Radioanalytical and Nuclear Chemistry,* 268(3), 503-509. Wiley). doi: https://doi.org/10.1007/s10967-006-0198-2

[34] Agüero, A., Pinedo, P., Simón, I., Cancio, D., Moraleda, M., Trueba, C., & Perez-Sanchez, D. (2008). Application of the Spanish Methodological Approach for Biosphere Assessment to a Generic High-level Waste Disposal Site. *Science of the Total Environment,* 403(1), 34-58. doi: https://doi.org/10.1016/j.scitotenv.2008.04.054

[35] Mavroulidou, M., Hughes, S. J., & Hellawell, E. E. (2004). A Qualitative Tool Combining an Interaction Matrix and a GIS to Map Vulnerability to Traffic Induced Air Pollution. *Journal of Environmental Management,* 70(4), 283-289. doi: https://doi.org/10.1016/j.jenvman.2003.12.002

[36] Condor, J., & Asghari, K. (2009). An Alternative Theoretical Methodology for Monitoring the Risks of CO< sub> 2</sub> Leakage from Wellbores. *Energy Procedia,* 1(1), 2599-2605.

[37] Fattahi, H., & Moradi, A. (2017) Risk assessment and estimation of TBM penetration rate using RES-based model. *Geotech Geol Eng* 35:365–

[38] Fattahi, H. (2017) Risk assessment and prediction of safety factor for circular failure slope using rock engineering systems. *Environ Earth Sci* 76:224

[39] Fattahi, H. (2018). Applying Rock Engineering Systems to Evaluate Shaft Resistance of a Pile Embedded in Rock. *Geotechnical and Geological Engineering.* https://doi.org/10.1007/s10706-018-0536-5

[40] Fattahi, H., & Moradi, A. (2018) A new approach for estimation of the rock mass deformation modulus: a rock engineering systems-based model. *Bull Eng Geol Environ* 77, 363–374.

[41] Huang, R., Huang, J., Ju, N., & Li, Y. (2013) Automated tunnel rock classification using rock engineering systems. *Eng Geol.* 156, 20–27

[42] Fattahi, H. (2018) An estimation of required rotational torque to operate horizontal directional drilling using rock engineering systems. *J Pet Sci Technol* 8:82–96.

[43] Faramarzi, F, Mansouri, H., & Ebrahimi-Farsangi, M. A. (2014). Development of rock engineering systems-based models for fly rock risk analysis and prediction of flyrock distance in surface blasting. *Rock Mechanics and Rock Engineering,* 47, 1291–1306. doi: https://doi.org/10.1007/s00603-013-0460-1

[44] Saffari, A., Sereshki, F., Ataei, M. & Ghanbari, K. (2013). Applying Rock Engineering Systems (RES) approach to Evaluate and Classify the Coal Spontaneous Combustion Potential in Eastern Alborz Coal Mines. *Int. J. Min.& Geo-Eng.,* 47(2), 115-127. https://doi.org/10.22059/ijmge.2013.51333

[45] Hudson, J. A. (1992). Rock engineering systems: theory and practice. Ellis Horwood, Chichester.

[46] Mazzoccola, D. F., & Hudson, J. A. (1996). A Comprehensive Method of Rock Mass Characterization for Indicating Natural Slope Stability. *Quarterly Journal of Engineering Geology;* 29, 37 – 56. doi: http://qjegh.lyellcollection.org/

[47] Yang, Y., & Zhang, Q. (1998). The application of neural networks to rock engineering systems (RES). *International Journal of Rock Mechanics and Mining Science,* 35, 727–745. doi: doi: https://doi.org/10.1016/S0148-9062(97)00339-2

[48] Zare-Naghadehi, M., Jimenez, R., KhaloKakaie, R., & Jalali, S. M. E. (2011). A probabilistic systems methodology to analyze the importance of factors affecting the stability of rock slopes. *Eng. Geol.;* 118, 82–92. doi: https://10.1016/j.enneo.2011.01.003

[49] Zare-Naghadehi, M., Jimenez, R., KhaloKakaie, R., & Jalali, S. M. E. (2013). A new open-pit mine slope instability index defined using the improved rock engineering systems approach. *International Journal of Rock Mechanics and Mining Science,* 61, 1–14. doi: http://dx.doi.org/10.1016/j.ijrmms.2013.01.012

[50] Frough, O., & Torabi, S. R. (2013). An application of rock engineering systems for estimating TBM downtimes. *Engineering Geology,* 157, 112–123. doi: https://dx.doi.org/10.1016/j.enggeo.2013.02.003

[51] Faramarzi, F., Ebrahimi Farsangi, M. A. & Mansouri, H. (2013). An RES based model for risk assessment and prediction of back break in bench blasting. Rock Mech Rock Eng.; 46, pp.877–887. https://dx.doi.org/10.1016/j.ijrmms.2012.12.045

[52] Hudson, J. A. (2013). Review of Rock Engineering Systems applications over the last 20 years. In Rock Characterisation, Modelling and Engineering Design Methods. *Taylor & Francis Group: London, UK,* 419–424. doi: https://dx.doi.org/10.1201/b14917-75

[53] Jiao, Y., & Hudson, J. A. (1998). Identifying the critical mechanism for rock engineering design. *Géotechnique,* 48, 319–335.

[54] Benardos, A. G., & Kaliampakos, D. C. (2004): A Methodology for Assessing Geotechnical Hazards for TBM Tunnelling—Illustrated by the Athens Metro, Greece. *International Journal of Rock Mechanics and Mining Sciences,* 4, 987–999. doi: https://doi.10.1016/j.ijrmms.2004.03.007

[55] Mohammadi. M., & Azad, A. (2020). Applying Rock Engineering Systems Approach for Prediction of Overbreak Produced in Tunnels Driven in Hard Rock. *Geotechnical and Geological Engineering,* 38, 2447–2463. doi: https://doi.org/10.1007/s10706-019-01161-z

[56] Singh, P. K., Roy, M. P., Paswan, R. K., Sarim, Md., Kumar, S., &

Jha, R. R. (2015). Rock fragmentation control in opencast blasting. *Journal of Rock Mechanics and Geotechnical Engineering,* 8(2), 225-237. doi: https://doi.org/10.1016/j.jrmge.2015.10.005

[57] Armaghani, D. J., Hajihassani, M., Mohamad, E. T., Marto, A., & Noorani, S. A. (2014). Blasting-induced flyrock and ground vibration prediction through an expert artificial neural network based on particle swarm optimization. *Arabian Journal of Geosciences,* 7(12), 5383–5396. doi: https://doi.org/10.1007/s12517-013-1174-0

[58] Konya, C. J., & Walter, E. J. (1990). Surface blast design. New Jersey: Prentice Hall.

[59] Salmi, E. F., & Sellers, E. J. (2021). A review of the methods to incorporate the geological and geotechnical characteristics of rock masses in blastability assessments for selective blast design. *Engineering Geology,* 281, 105970. doi: https://doi.org/10.1016/j.enggeo.2020.105970

[60] Cunningham, C. V. B. (1983). The Kuz-Ram model for prediction of fragmentation from blasting. In: Proceedings of the first international symposium on rock fragmentation by blasting. Lulea, Sweden; 23–26 August 1983. p. 439-453.

[61] Hasanipanah, M., Armaghani, D. J., Monjezi, M., & Shams, S. (2016). Risk Assessment and Prediction of Rock Fragmentation Produced by Blasting Operation: A Rock Engineering System. *Environmental Earth Sciences*, 75, 1–12. doi: https://doi.10.1007/s12665-016-5503-y